Available online at www.sciencedirect.com

ScienceDirect

Nuclear Physics B 906 (2016) 60–76

NUCLEAR PHYSICS B

www.elsevier.com/locate/nuclphysb

Bottom quark contribution to spin-dependent dark matter detection

Jinmian Li *, Anthony W. Thomas

ARC Centre of Excellence for Particle Physics at the Terascale (CoEPP), and CSSM, Department of Physics, University of Adelaide, South Australia 5005, Australia

Received 7 December 2015; received in revised form 24 February 2016; accepted 2 March 2016

Available online 7 March 2016

Editor: Hong-Jian He

Abstract

We investigate a previously overlooked bottom quark contribution to the spin-dependent cross section for Dark Matter (DM) scattering from the nucleon. While the mechanism is relevant to any supersymmetric extension of the Standard Model, for illustrative purposes we explore the consequences within the framework of the Minimal Supersymmetric Standard Model (MSSM). We study two cases, namely those where the DM is predominantly Gaugino or Higgsino. In both cases, there is a substantial, viable region in parameter space ($m_{\tilde{b}} - m_{\chi} \lesssim \mathcal{O}(100)$ GeV) in which the bottom contribution becomes important. We show that a relatively large contribution from the bottom quark is consistent with constraints from spin-independent DM searches, as well as some incidental model dependent constraints.

1. Introduction

The existence of non-baryonic Dark Matter (DM) has been established by many astronomical observations [1,2]. Amongst the many candidates for DM, the so-called Weakly Interacting Massive Particles (WIMPs), which would have a mass in the range $\mathcal{O}(1)$ GeV–$\mathcal{O}(1)$ TeV, are one of the most attractive. These particles would only interact with Standard Model (SM)

* Corresponding author.
E-mail address: jinmian.li@adelaide.edu.au (J. Li).

http://dx.doi.org/10.1016/j.nuclphysb.2016.03.003

particles through weak interactions (and gravity), in order to yield a DM relic density consistent with measurement $\Omega_{\rm DM}h^2 = 0.1199 \pm 0.0027$ [3].

Direct detection of DM relies on observing the recoil energy after scattering from normal matter through weak interactions. Several DM direct detection experiments have claimed a possible excess, namely DAMA [4], CoGeNT [5], CRESST [6] and CDMS [7]. On the other hand, these results are challenged by the absence of signals at XENON100 [8] and LUX [9], as well as CDMSlite [10] in the light DM region. The coherent, spin-independent (SI) interaction between a DM particle, generically labelled χ, and a nucleus is proportional to the nucleon number. Because of the relatively heavy nuclei chosen for most of the above mentioned experiments, both the observed excess and stringent exclusion limits are based on SI χ–p scattering.

As for spin-dependent (SD) DM detection [11], in a simple shell model the spin of the nucleus is that of a single, unpaired nucleon. As a consequence, the matrix element for SD χ-nucleus scattering will be roughly comparable with that for SI χ-nucleon scattering, with no enhancement by the nucleon number. As a result, the current DM direct searches place only very loose bounds on the SD cross section [12–14].

In the standard calculation of SD DM-nucleon scattering the heavy quark contribution is usually neglected. That is, only the contributions from Δu, Δd and Δs are included. However, as explained in the context of the proton weak charge [15], the usual decoupling of heavy quarks through the Appelquist–Carrazone theorem [16] does not apply to quantities influenced by the $U(1)$ axial anomaly [17–21]. In that case, rather than being suppressed by inverse powers of the heavy quark mass, the suppression is only logarithmic. These logarithmic corrections were studied in considerable detail by Bass et al. in Refs. [15,22,23], at both leading and next-to-leading order. As we shall explain here, there are interesting scenarios of supersymmetry (SUSY), generally involving a relatively light sbottom, where the logarithmic radiative correction involving the b-quark that is further enhanced by resonant effect may make a significant contribution to SD DM-nucleon scattering.

Indeed, SUSY [24,25] is widely believed to provide the most promising explanation for new physics beyond SM. In SUSY models with R-parity conservation, the lightest supersymmetric particle (LSP) is stable and can become a DM candidate. On the other hand, both the LHC SUSY searches [26,27] and naturalness arguments [28,29] suggest that only the third generation supersymmetric quarks (squarks) can be light. In Ref. [30], it has been argued that an sbottom with a mass as light as $\sim \mathcal{O}(15)$ GeV might still be consistent with current searches. In other models, such as the simplified model framework [31] and flavored DM models [32,33], the DM can only couple to the bottom quark, as motivated by the recent DM indirect signals [34]. Studying the bottom quark contribution to the DM-nucleon SD cross section is crucial in models of this type.

In this work, we focus on the Minimal Supersymmetric Standard Model (MSSM) with a relatively light sbottom, showing when and how the bottom contribution becomes important. When the DM is Wino, there is no coupling between DM and the Z-boson and only squark mediated processes can contribute to χ-nucleon scattering. We investigate the parameter space where the sbottom contribution is comparable to, or larger than, the first generation squark contribution. When the DM is Higgsino, the first two generation squark mediated processes are greatly suppressed by their small Yukawa couplings. However, the Higgsino can couple to the Z-boson. The constructive and destructive interference effects between Z and sbottom ($\tilde{b}$) mediated processes are discussed in detail for a number of variations on the structure of the neutralino.

Any sbottom mediated process that contributes to the SD scattering cross section can also contribute to SI scattering. We consider the stringent LUX constraint on SI DM detection for light sbottom scenarios of interest. A relatively large SD bottom contribution can indeed be

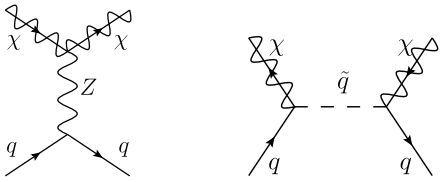

Fig. 1. Processes that contribute to the Dark Matter spin dependent cross section for scattering from a nucleon.

found, while maintaining consistency with the LUX constraint. We also consider several model dependent constraints from collider searches. We stress that our conclusion has implications beyond the MSSM, which is used here purely for purposes of illustration.

This paper is organised as follows. In Sec. 2, we explain the theoretical framework for the calculation of the SD DM-nucleon scattering cross section. Sec. 3 discusses the bottom contribution for Wino and Higgsino DM. The corresponding SI detection and LHC constraints on the light sbottom scenario are considered in Sec. 4 and Sec. 5. In Sec. 6 we present some concluding remarks.

2. Effective interaction for Spin-Dependent DM-nucleon scattering in MSSM

Given a general effective Lagrangian

$$\mathcal{L}_{\rm SD}^{\rm eff} = d_q \bar{\chi}\gamma^\mu\gamma_5\chi\bar{q}\gamma_\mu\gamma_5 q \ , \tag{1}$$

the spin-dependent χ-nucleon scattering cross section can be written as

$$\sigma_{\rm SD}^{p,n} = \frac{12}{\pi}\left(\frac{m_\chi m_{p,n}}{m_\chi + m_{p,n}}\right)^2 |a_{p,n}|^2 \ , \tag{2}$$

where

$$a_{p,n} = \sum_q d_q \Delta q_{p,n} \ . \tag{3}$$

The factors $\Delta q_{p,n}$ parameterise the corresponding quark spin content of the nucleon:

$$2s_\mu \Delta q_N = < N|\bar{\psi}_q\gamma_\mu\gamma_5\psi_q|N > \ , \tag{4}$$

where s_μ is the nucleon spin. The preferred values of the light quark contributions in the proton and neutron are:

$$\begin{aligned} &\Delta_u^{(p)} = \Delta_d^{(n)} = 0.84, \ \ \Delta_d^{(p)} = \Delta_u^{(n)} = -0.43, \\ &\Delta_s^{(p)} = \Delta_s^{(n)} = -0.02 \ , \end{aligned} \tag{5}$$

where the strange quark contribution is motivated by a recent lattice QCD calculation [35].

In the MSSM at tree level, there are two processes which can contribute to the effective Lagrangian. The corresponding Feynman diagrams are given in Fig. 1. From those processes, we are able to calculate the coefficients of the effective Lagrangian from the renormalisable Lagrangian below:

$$\mathcal{L} = \bar{q}(a_q + b_q\gamma_5)\chi\tilde{q} + c\bar{q}\gamma^\mu\gamma^5 q Z_\mu + d\bar{\chi}\gamma^\mu\gamma_5\chi Z_\mu \ . \tag{6}$$

The corresponding couplings in the MSSM are written as [36]

$$a_u = i\frac{Z^L_{\tilde{u}}}{2}\left(\frac{-g}{\sqrt{2}c_w}\left(\frac{1}{3}Z^{11}_N s_w + Z^{21}_N c_w\right) - Y_u Z^{41}_N\right) + i\frac{Z^R_{\tilde{u}}}{2}\left(\frac{2\sqrt{2}g s_w}{3c_w}Z^{11}_N - Y_u Z^{41}_N\right) \tag{7}$$

$$b_u = i\frac{Z^L_{\tilde{u}}}{2}\left(\frac{g}{\sqrt{2}c_w}\left(\frac{1}{3}Z^{11}_N s_w + Z^{21}_N c_w\right) - Y_u Z^{41}_N\right) + i\frac{Z^R_{\tilde{u}}}{2}\left(\frac{2\sqrt{2}g s_w}{3c_w}Z^{11}_N + Y_u Z^{41}_N\right) \tag{8}$$

$$a_d = i\frac{Z^L_{\tilde{d}}}{2}\left(\frac{-g}{\sqrt{2}c_w}\left(\frac{1}{3}Z^{11}_N s_w - Z^{21}_N c_w\right) + Y_d Z^{31}_N\right) + i\frac{Z^R_{\tilde{d}}}{2}\left(\frac{-\sqrt{2}g s_w}{3c_w}Z^{11}_N + Y_d Z^{31}_N\right) \tag{9}$$

$$b_d = i\frac{Z^L_{\tilde{d}}}{2}\left(\frac{g}{\sqrt{2}c_w}\left(\frac{1}{3}Z^{11}_N s_w - Z^{21}_N c_w\right) + Y_d Z^{31}_N\right) + i\frac{Z^R_{\tilde{d}}}{2}\left(\frac{-\sqrt{2}g s_w}{3c_w}Z^{11}_N - Y_d Z^{31}_N\right) \tag{10}$$

$$c = \frac{i}{2}\frac{g}{c_w}T_{3q} \tag{11}$$

$$d = -\frac{i}{4}\frac{g}{c_w}((Z^{41}_N)^2 - (Z^{31}_N)^2) \tag{12}$$

We consider first the Z boson mediated amplitude in the non-relativistic limit:

$$\begin{aligned}\mathcal{M}^Z_{\rm SD} &= c\ d\ \bar{\chi}\gamma^\mu\gamma_5\chi\frac{-ig_{\mu\nu}}{Q^2 - m_Z^2}\bar{q}\gamma^\nu\gamma_5 q \\ &\sim c\ d\ \frac{i}{m_Z^2}(1 + \mathcal{O}(m_Z^{-2}))\bar{\chi}\gamma^\mu\gamma_5\chi\gamma_\mu\gamma_5 q \\ &\sim c\ d\ \frac{i}{m_Z^2}\bar{\chi}\gamma^\mu\gamma_5\chi\gamma_\mu\gamma_5 q\,,\end{aligned} \tag{13}$$

so that the effective coupling d_q in Eq. (1) is:

$$d_q = \frac{cd}{m_Z^2} = \frac{g^2}{4m_W^2}T_{3q}((Z^{41}_N)^2 - (Z^{31}_N)^2). \tag{14}$$

Next, for the $\tilde{q}$ mediated process we find:

$$\begin{aligned}\mathcal{M}^{\tilde{q}}_{\rm SD} &= \bar{\chi}(a - b\gamma_5)q\frac{i}{(p_\chi + p_q)^2 - m^2_{\tilde{q}}}\bar{q}(a + b\gamma_5)\chi \\ &\sim \frac{-i}{m^2_{\tilde{q}} - (m_\chi + m_q)^2}\bar{\chi}(a - b\gamma_5)q\ \bar{q}(a + b\gamma_5)\chi\end{aligned}$$

$$= \frac{-i}{m_{\tilde{q}}^2 - (m_\chi + m_q)^2}(a^2 \bar{\chi} q \ \bar{q}\chi - b^2 \bar{\chi}\gamma_5 q \ \bar{q}\gamma_5 \chi)$$

$$\ni \frac{-i}{m_{\tilde{q}}^2 - (m_\chi + m_q)^2}(\frac{a^2+b^2}{4} \bar{\chi}\gamma^\mu\gamma_5\chi \ \bar{q}\gamma_\mu\gamma_5 q)\,. \tag{15}$$

In this case the effective coupling in Eq. (1) is:

$$d_q = -\frac{1}{4}\frac{a^2+b^2}{m_{\tilde{q}}^2 - (m_\chi + m_q)^2}\,. \tag{16}$$

Note that the tree level effective coupling d_q is only reliable when $m_{\tilde{q}} - m_\chi$ is significantly larger than m_q. Some discussions regarding the precision of the tree level approximation are given in Appendix A. And we have also checked that the result calculated from Eq. (16) matches well with numerical tool micrOMEGAs for light flavor quark.

3. Light sbottom contribution

For most processes of physical interest the Appelquist–Carrazone theorem tells us that heavy quark contributions are suppressed by order $1/m_Q^2$. However, as explained in the introduction, because of the $U(1)$ axial anomaly, the heavy quark contributions to spin-dependent quantities are only logarithmically suppressed. The particular case where this has been explored in great detail is the neutral weak charge of the proton. Without heavy quarks this is just $\Delta u - \Delta d - \Delta s$, which has been used to infer values of Δs. However, for a precise determination one must include the radiative corrections involving heavy quark loops which enter at order $1/\ln m_Q$. For example, one finds a LO correction from the b-quark equal to [15]:

$$\Delta_b^{(p)} = -\frac{6}{23\pi}\tilde{\alpha}_b(\Delta_u^{(p)} + \Delta_d^{(p)} + \Delta_s^{(p)}) \sim -0.0066\,. \tag{17}$$

We note that Eq. (17) is second order in the strong coupling at the b mass, as is evident in the residual 5-flavor factor 6/23 appearing there. However, the regularisation of the triangle diagram leads to a logarithm in m_b in the numerator which has been used to cancel the logarithm in one factor of $\tilde{\alpha}_b$. The logarithmic radiative correction $\Delta_b^{(p)}$ is around 2 order of magnitude below the $\Delta_u^{(p)}$. We will show later that with further enhancement from resonant effect the contribution from $\Delta_b^{(p)}$ can easily become dominant in the spin-dependent χ-nucleon scattering.

Provided that the difference between the sbottom mass and that of the DM candidate is significantly larger than the mass of the b-quark, the $\tilde{q}$ propagator in Fig. 1 can be effectively factored out, leaving the familiar triangle diagram which involves the $U(1)$ axial anomaly. In this case the bottom contribution to the axial charge of the target proton can be taken directly from Eq. (17). We shall take the running coupling $\tilde{\alpha}_b = 0.2$. As a result, for the Z-mediated process, the contribution of $\Delta_b^{(p)}$ can only change the result by a factor of

$$(\frac{\Delta_u^{(p)} - \Delta_d^{(p)} - \Delta_s^{(p)} - \Delta_b^{(p)}}{\Delta_u^{(p)} - \Delta_d^{(p)} - \Delta_s^{(p)}})^2 \sim 1.01\,, \tag{18}$$

which is clearly very small.

On the other hand, the term involving $\Delta_b^{(p)}$ can give a significant contribution to the spin-dependent χ-nucleon cross section when $\tilde{b}$ is relatively close in mass to the DM candidate, i.e.

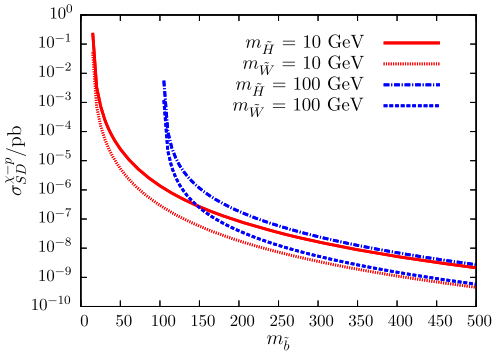

Fig. 2. Sbottom contribution to the SD scattering cross section for Wino and Higgsino Dark Matter from the proton.

with resonant enhancement. For simplicity we study the cases where the DM particle is either pure Wino or pure Higgsino. The corresponding couplings are:

$$a_b^{(\tilde{W})} = \frac{ig}{2\sqrt{2}} Z_{\tilde{b}}^L, \quad a_b^{(\tilde{H})} = \frac{i}{2} Y_b Z_N^{31} (Z_{\tilde{b}}^L + Z_{\tilde{b}}^R) \tag{19}$$

$$b_b^{(\tilde{W})} = -\frac{ig}{2\sqrt{2}} Z_{\tilde{b}}^L, \quad b_b^{(\tilde{H})} = \frac{i}{2} Y_b Z_N^{31} (Z_{\tilde{b}}^L - Z_{\tilde{b}}^R) \tag{20}$$

where $Y_b = \frac{g}{\sqrt{2} m_W \cos\beta} m_b$. So, the cross section can be written as

$$\sigma_{\rm SD}^{\tilde{b}-\tilde{W}} = \frac{12}{\pi} \left(\frac{m_\chi m_p}{m_\chi + m_p}\right)^2 \left(-\frac{g^2 (T_{3b} Z_{\tilde{b}}^L)^2}{4(m_{\tilde{b}}^2 - (m_\chi + m_b)^2)} \Delta_b^{(p)}\right)^2 \tag{21}$$

$$\sigma_{\rm SD}^{\tilde{b}-\tilde{H}} = \frac{12}{\pi} \left(\frac{m_\chi m_p}{m_\chi + m_p}\right)^2 \left(-\frac{0.5 Y_b^2 (Z_N^{31})^2}{4(m_{\tilde{b}}^2 - (m_\chi + m_b)^2)} \Delta_b^{(p)}\right)^2 \tag{22}$$

where we have assumed the gauge eigenstate limit and only the sbottom mediated process is contributing. By fixing m_χ at either 10 or 100 GeV and taking $Z_{\tilde{b}}^L = 1$ and $\tan\beta = 40$, $Z_N^{31} = \frac{1}{\sqrt{2}}$ for Wino and Higgsino DM, respectively, we can calculate the corresponding cross section as a function of $m_{\tilde{b}}$. The result is shown in Fig. 2. From Fig. 2 we see that the sbottom can give a very large contribution when the mass splitting $m_{\tilde{b}} - m_\chi$ is $\lesssim 100$ GeV.

3.1. Comparison with the contribution from the first generation squarks

First, we study the simpler case where the DM is gaugino. In this case there is no coupling between the Z boson and DM and only the squark mediated process can contribute to the SD interaction. In this subsection, we investigate the extent to which the sbottom should be lighter than first generation squark, so that they at least have comparable cross sections. In the following we consider the sum of the contributions of all first generation squarks ($\tilde{u}_L$, $\tilde{u}_R$, $\tilde{d}_L$, $\tilde{d}_R$), with their masses taken to be degenerate for simplicity.

Assuming that the DM is either pure Wino or Bino, the ratio of the corresponding SD cross section for sbottom to the sum of the contributions from all the first generation squarks can be calculated as

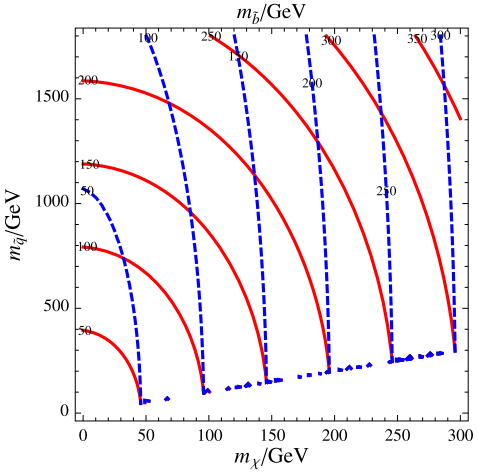

Fig. 3. Contours of constant $m_{\tilde{b}}$ which show where the sbottom and degenerate first generation squarks give the same contribution for Wino (red solid line) and Bino (blue dashed line) DM. (For interpretation of the references to colour in this figure legend, the reader is referred to the web version of this article.)

$$\frac{\sigma_{\rm SD}^{\tilde{b}-\tilde{W}}}{\sigma_{\rm SD}^{\tilde{q}_{u,d}-\tilde{H}}} = \frac{(Z_{\tilde{b}}^L)^2|\Delta_b^{(p)}|}{m_{\tilde{b}}^2-(m_\chi+m_b)^2} \Big/ \frac{\Delta_u^{(p)}+\Delta_d^{(p)}}{m_{\tilde{q}_{u,d}}^2-m_\chi^2} \tag{23}$$

$$\frac{\sigma_{\rm SD}^{\tilde{b}-\tilde{B}}}{\sigma_{\rm SD}^{\tilde{q}_{u,d}-\tilde{B}}} = \frac{(a^2+b^2)_{\tilde{b}_1}}{m_{\tilde{b}}^2-(m_\chi+m_b)^2} \times \left(\frac{\sum_{\tilde{u}_{L,R}}(a^2+b^2)\Delta_u^{(p)}+\sum_{\tilde{d}_{L,R}}(a^2+b^2)\Delta_d^{(p)}}{m_{\tilde{q}_{u,d}}^2-m_\chi^2}\right)^{-1}. \tag{24}$$

The corresponding contours of $\sigma_{\rm SD}^{\tilde{b}-\chi} = \sigma_{\rm SD}^{\tilde{q}_{u,d}-\chi}$ are shown in Fig. 3. The case of Wino DM is more interesting than that of Bino DM because of its larger g_2 coupling. In this case, for 1.5 TeV first generation squarks and $\mathcal{O}(100)$ GeV DM, an sbottom lighter than about 200 GeV gives a larger cross section than the first generation squarks. On the other hand, for Bino DM, a much lighter sbottom ($\sim$ 110 GeV) is required – too light for the present calculation to be reliable.

3.2. *Contribution coherent with that of the Z-boson*

When the DM is predominantly Higgsino, the first two generation squark mediated processes are greatly suppressed by their small Yukawa couplings. Its couplings to the Z boson and sbottom are dependent on the mixing between the two Higgsino states.

Firstly, we briefly discuss the Higgsino mixing in the MSSM. In the basis ($\tilde{B}$, $\tilde{W}$, $\tilde{H}_d^0$, $\tilde{H}_u^0$), the neutralino mass matrix is given by:

$$M_N = \begin{pmatrix} M_1 & 0 & -c_\beta s_W m_Z & s_\beta s_W m_Z \\ 0 & M_2 & c_\beta c_W m_Z & -s_\beta c_W m_Z \\ -c_\beta s_W m_Z & c_\beta c_W m_Z & 0 & -\mu \\ s_\beta s_W m_Z & -s_\beta c_W m_Z & -\mu & 0 \end{pmatrix} \tag{25}$$

From the mass matrix we conclude that if

$$m_Z \ll \mu, M_1, M_2 \,, \tag{26}$$

the four neutralino mass eigenstates $\tilde{N}_i$ will be Bino $\tilde{B}$ dominated, Wino $\tilde{W}$ dominated and Higgsino $(\tilde{H}_u^0 \pm \tilde{H}_d^0)/\sqrt{2}$ dominated, respectively. For example, if we also decouple the Bino and Wino from the mass matrix, the component difference between $\tilde{H}_u^0$ and $\tilde{H}_d^0$, for a given mass eigenstate is

$$\Delta N_{\tilde{H}_u^0 - \tilde{H}_d^0} \propto \frac{m_Z^2}{M_i \mu} \tag{27}$$

For a few TeV gaugino and a few hundred GeV Higgsino, $\Delta N_{\tilde{H}_u^0 - \tilde{H}_d^0} \sim \mathcal{O}(10^{-2})$. Then, the contribution from the Z boson mediated process can be estimated by

$$\begin{aligned}\sigma_{\rm SD}^Z &= \frac{12}{\pi}\left(\frac{m_\chi m_p}{m_\chi + m_p}\right)^2 \Big(\sum_{q=u,d,s} d_q \Delta q^{(p)} \Big)^2 \\ &= \frac{12}{\pi}\left(\frac{m_\chi m_p}{m_\chi + m_p}\right)^2 \left(\frac{g^2}{8 m_W^2}((Z_N^{41})^2 - (Z_N^{31})^2)\right)^2 \qquad (28) \\ &\left(\Delta_u^{(p)} \times \frac{1}{2} + \Delta_d^{(p)} \times \left(-\frac{1}{2}\right) + \Delta_s^{(p)} \times \left(-\frac{1}{2}\right)\right)^2 \,, \qquad (29)\end{aligned}$$

which is $\sim 10^{-6}$ pb. From Fig. 2, we conclude that this corresponds to $m_{\tilde{b}} \sim 150$ GeV for $m_\chi \sim 100$ GeV.

To have a closer look at the coherent effects of Z boson and sbottom mediated processes, we have chosen the decoupled Wino/Bino limit, with the Higgsino DM mixing:

$$\chi = a \tilde{H}_d + b \tilde{H}_u \,, \tag{30}$$

where $a^2 + b^2 = 1$ and $b = 1.01a$, as argued previously. This corresponds to a cross section for the Z mediated process of order $\sim 3 \times 10^{-6}$ pb.

In this region, the $\tilde{b}$ mediated process may also give a competitive contribution. As a result, the DM will have opposite sign coherent effects for the proton and neutron:

$$\begin{aligned}\sigma_{\rm SD}^{\chi-(p,n)} &= \frac{12}{\pi}\left(\frac{m_\chi m_p}{m_\chi + m_p}\right)^2 \Big(\Big(\frac{g^2((Z_N^{41})^2 - (Z_N^{31})^2)}{8 m_W^2}\Big)\Big(T_{3u}\Delta_u^{(p,n)} \\ &+ T_{3d}\Delta_d^{(p,n)} + T_{3s}\Delta_s^{(p,n)}\Big) - \frac{0.5 Y_b^2 (Z_N^{31})^2}{4(m_{\tilde{b}}^2 - (m_\chi + m_b)^2)}\Delta_b^{(p,n)}\Big)^2 \,. \qquad (31)\end{aligned}$$

This makes the detailed consequences for SD DM scattering from real nuclei [37] potentially very complex.

We show the importance of the b-quark contribution through its coherent effects between Z mediated and sbottom mediated processes in Fig. 4. There we have marked out the compressed spectrum region ($\Delta(m_{\tilde{b}} - m_\chi) \lesssim 20$ GeV) where our tree level calculation cannot be considered reliable. According to the Eq. (31) with assumed $Z_N^{41} = 1.01 Z_N^{31}$, the first term in the parenthesis is positive for proton and negative for neutron, while the second term is always negative because $\Delta_b^{(p)} = \Delta_b^{(n)} < 0$. As a result, the interference terms for proton and neutron are constructive and destructive, respectively. We find that for the DM mass around $\mathcal{O}$(10–100) GeV an sbottom with mass $\lesssim 300$ GeV can make a non-negligible contribution. In some specific regions, the corresponding cross section for the Z-mediated process may even be enhanced or reduced by several orders of magnitude.

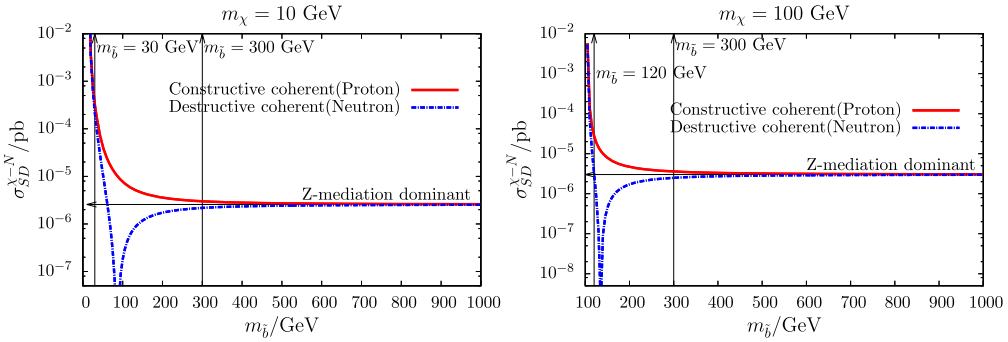

Fig. 4. Constructive and destructive coherence effects between Z mediated and $\tilde{b}$ mediated processes for $m_\chi = 10$ GeV (left) and $m_\chi = 100$ GeV (right), respectively. The vertical arrowed lines at $m_{\tilde{b}} = 30$ GeV and $m_{\tilde{b}} = 120$ GeV indicate the value below which the calculation should not be considered reliable.

4. Spin-independent DM detection constraint from LUX

The same process shown in the right panel of Fig. 1, which can give rise to an enhancement of the spin-dependent scattering cross section, can also contribute to spin-independent scattering. As a result, the very stringent spin-independent DM search bound from LUX [9] may already exclude some of the parameter region found to be of interest here.

We start with the following effective Lagrangian [38–41]:

$$\mathcal{L}_{\rm SI} = \sum_q (f_q m_q \bar{\chi}\chi\bar{q}q + \frac{g_q^{(1)}}{m_\chi}\bar{\chi} i\partial^\mu \gamma^\nu \chi \mathcal{O}^q_{\mu\nu} + \frac{g_q^{(2)}}{m_\chi^2}\bar{\chi}(i\partial^\mu)(i\partial^\nu)\chi\mathcal{O}^q_{\mu\nu}) + f_G \bar{\chi}\chi G^a_{\mu\nu}G^{a\mu\nu} \tag{32}$$

where χ is the DM field, m_χ its mass and the twist-2 operator:

$$\mathcal{O}^q_{\mu\nu} = \frac{1}{2}\bar{q} i (D_\mu \gamma_\nu + D_\nu \gamma_\mu - \frac{1}{2} g_{\mu\nu} \not{D}) q \ . \tag{33}$$

The corresponding spin-independent scattering cross section of DM with a proton can be written as

$$\sigma^{\chi-p}_{\rm SI} = \frac{4}{\pi}\mu^2 (f_N)^2 \tag{34}$$

where $\mu = m_\chi m_N/(m_\chi + m_N)$ and

$$\frac{f_N}{m_N} = \sum_{q=u,d,s} f_q f_{T_q} + \sum_{q=u,d,s,c,b} \frac{3}{4}(q(2)+\bar{q}(2))(g_q^{(1)}+g_q^{(2)}) - \frac{8\pi}{9\alpha_s} f_{T_G} f_G \tag{35}$$

$$\sim \sum_{q=u,d,s} f_q f_{T_q} + \sum_{q=u,d,s,c,b} \frac{3}{4}(q(2)+\bar{q}(2))(g_q^{(1)}+g_q^{(2)}) + \frac{2}{27}\sum_{Q=c,b,t} f_{T_G} f_Q \tag{36}$$

The light quark parameters f_{T_q} are defined by

$$f_{T_q} m_N = < N|m_q \bar{q} q|N > \ , \tag{37}$$

and $f_{T_G} = 1 - \sum_{q=u,d,s} f_{T_q}$. Recent lattice simulations give [42–45]:

$$f_u^p = 0.023, \quad f_d^p = 0.033, \quad f_s^p = 0.026 \ . \tag{38}$$

The second moments of the parton distribution functions (PDFs) can be used to evaluate the matrix element of $\mathcal{O}^q_{\mu\nu}$:

$$(p_\mu p_\nu - \frac{1}{4} m_N^2 g_{\mu\nu})(q(2) + \bar{q}(2)) = m_N < N(p)|\mathcal{O}^q_{\mu\nu}|N(p) > , \tag{39}$$

which from the CTEQ PDFs [46] yields

$$b(2) = 0.012, \quad \bar{b}(2) = 0.012 \ , \tag{40}$$

at the Z boson mass scale.

Using a similar technique to that used in calculating the SD effective coefficient, d_q, above, we can find the corresponding effective coefficient for the spin-independent case. Based on the renormalizable Lagrangian Eq. (6), we have

$$\begin{aligned} f_q = & \frac{m_\chi}{(m_{\tilde{q}}^2 - (m_\chi + m_q)^2)^2} \frac{a_q^2 + b_q^2}{8} \\ & - \frac{1}{m_q (m_{\tilde{q}}^2 - (m_\chi + m_q)^2)} \frac{a_q^2 - b_q^2}{4} \end{aligned} \tag{41}$$

$$g_q^{(1)} + g_q^{(2)} = \frac{m_\chi}{(m_{\tilde{q}}^2 - (m_\chi + m_q)^2)^2} \frac{a_q^2 + b_q^2}{2} \, . \tag{42}$$

As a result the twist-2 operator, $\mathcal{O}^q_{\mu\nu}$, gives a much larger contribution than f_q in most cases. For Higgsino DM, where $a_q \neq b_q$, the second term of f_q can easily become dominant. However in this case it is negative, so a cancellation between f_q and g_q may happen in some of the parameter regions.

We first consider the pure Wino DM case, with only $\tilde{b}_L$ mediated scattering. From Eq. (36), we have

$$f_N = m_p (\frac{3}{4}(b(2) + \bar{b}(2))(g_b^{\tilde{b}_L - \tilde{W}}) + \frac{2}{27} f_{T_G} f_b^{\tilde{b}_L - \tilde{W}}) \tag{43}$$

where

$$f_b^{\tilde{b}_L - \tilde{W}} = \frac{g^2 m_\chi}{32} \frac{1}{(m_{\tilde{b}}^2 - m_\chi^2)^2} \tag{44}$$

$$g_b^{\tilde{b}_L - \tilde{W}} = \frac{g^2 m_\chi}{8} \frac{1}{(m_{\tilde{b}}^2 - m_\chi^2)^2} \tag{45}$$

The tree level calculation for the spin-independent and spin-dependent cross sections is shown in Fig. 5. We conclude from the figure that $m_{\tilde{b}} - m_\chi \gtrsim 50$ GeV is required to evade the spin-independent bound from LUX for Wino DM. It has to be noted that the pole at $m_{\tilde{b}} = m_b + m_\chi$, for SI tree level results, will not show up when the full NLO effects are taken into account [47].

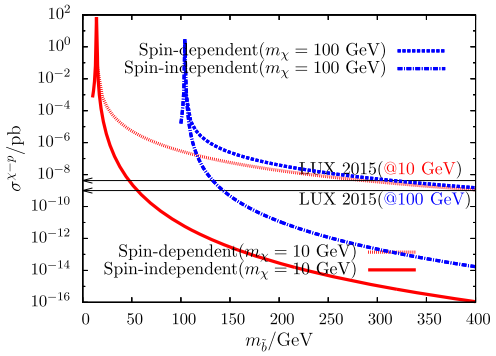

Fig. 5. SD and SI scattering cross section for Wino DM from the proton, with $m_\chi = 10$ GeV and $m_\chi = 100$ GeV, respectively.

We have checked that our results fit the numerical results from micrOMEGAs [48,49] quite well, outside the pole region.

Next, we discuss the more interesting case where the DM is predominantly Higgsino. As discussed above, in this case the relatively large spin dependent cross section from the sbottom mediated process can interfere coherently with the Z mediated process, leading to very different SD scattering rates for protons and neutrons.

The SI DM-proton effective coupling is

$$f_N = m_p\left(\frac{3}{4}(b(2)+\bar{b}(2))(g_b^{\tilde{b}_1-\tilde{H}}) + \frac{2}{27} f_{T_G} f_b^{\tilde{b}_1-\tilde{H}}\right) \tag{46}$$

where

$$f_b^{\tilde{b}_1-\tilde{H}} = \frac{m_\chi}{(m_{\tilde{b}}^2-(m_\chi+m_b)^2)^2}\frac{0.5Y_b^2(Z_N^{31})^2}{8} - \frac{1}{m_b(m_{\tilde{b}}^2-(m_\chi+m_b)^2)}\frac{Y_b^2(Z_N^{31})^2 Z_{\tilde{b}}^L Z_{\tilde{b}}^R}{4} \tag{47}$$

$$g_b^{\tilde{b}_1-\tilde{H}} = \frac{m_\chi}{(m_{\tilde{b}}^2-(m_\chi+m_b)^2)^2}\frac{0.5Y_b^2(Z_N^{31})^2}{2}\,. \tag{48}$$

The corresponding tree level calculation for the spin-dependent and spin-independent cross sections is shown in Fig. 6. From that figure we see that a small component of left-handed sbottom is favoured in order to evade the LUX bound. When the left-handed sbottom component is relatively large, a large SD cross section may also be consistent with the LUX experiment if there is a cancellation in $\sigma_{\rm SI}$.

5. Model dependent constraints and a general argument

We have presented a representative study of the potential importance of the bottom quark contribution to DM spin-dependent detection within the framework of the MSSM. This particular contribution has hitherto been overlooked. However, in a realistic model such as MSSM, there are many other incidental constraints. We will briefly outline how these may be evaded, while keeping our discussion as general as possible in this section.

LEP placed a very stringent bound on the chargino mass ($m_{\tilde{H}^\pm(\tilde{W}^\pm)} > 92.4(91.9)$ GeV) [50]. Because for either Wino and Higgsino DM there is a charged partner (chargino), which has very

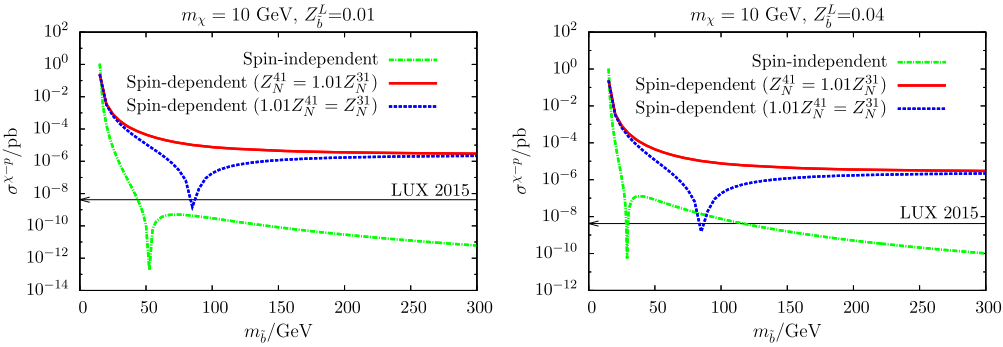

Fig. 6. SD and SI scattering cross section for different mixing of Higgsino DM from the proton. Left: $m_\chi = 10$ GeV, $Z_{\tilde{b}}^L = 0.01$. Right: $m_\chi = 10$ GeV, $Z_{\tilde{b}}^L = 0.04$.

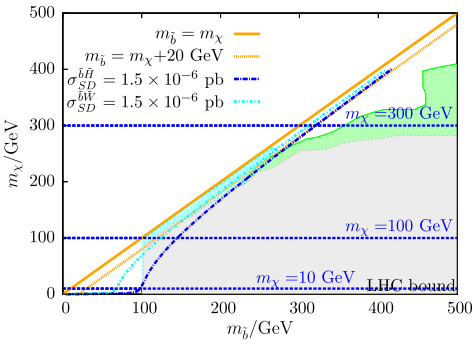

Fig. 7. LHC exclusion bound on sbottom mass versus DM mass. The grey, green and cyan shaded regions correspond to the exclusion limits given by LHC searches for sbottom at 8 TeV [51], 13 TeV [51] and searches for mono-jet at 8 TeV [53], respectively. (For interpretation of the references to colour in this figure legend, the reader is referred to the web version of this article.)

similar mass with the DM, we cannot have Wino and Higgsino DM of $m_\chi \lesssim 90$ GeV in a typical MSSM framework.

As for $m_\chi \gtrsim 100$ GeV, on the other hand, it will be constrained by LHC sbottom searches [51,52] and mono-jet search [53], since we usually need a relatively light sbottom to enhance the bottom quark spin dependent contribution. The corresponding LHC exclusion bounds and spin-dependent χ–p scattering cross section in the $m_{\tilde{b}}$–m_χ plane are shown in Fig. 7. To generate this figure we have used Eq. (21) and (22), where only the sbottom mediated process is considered. The contours of $\sigma_{\rm SD}^{\chi-p}$ show the condition when the sbottom mediated contribution is half the size of Z mediated process for Wino DM and a typical Higgsino DM candidate with $Z_N^{41} = 1.01 Z_N^{31}$. This figure suggests that a large portion of parameter space is excluded by the LHC sbottom searches.

However, there are several ways to avoid these constraints:

- For $m_\chi \lesssim 100$ GeV, we can work in a more general framework, where the dark matter does not have any charged partners. Its couplings to the Z boson and $\tilde{b}$ may be of the same order; e.g. the simplified model framework [31] or flavored dark matter models [32,33].

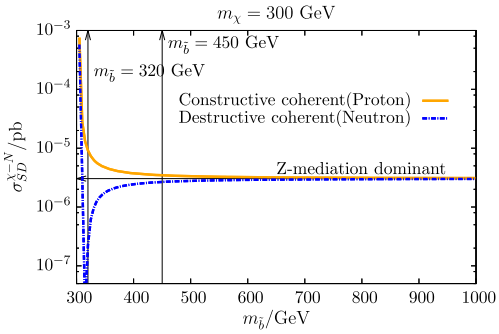

Fig. 8. Constructive and destructive interference effects between Z mediated and $\tilde{b}$ mediated processes for Higgsino DM with $m_\chi = 300$ GeV.

- For $m_\chi \lesssim 100$ GeV, if the charged Higgsino decays into DM and a relatively long lived particle, with lifetime of $\mathcal{O}$(10–100) cm, similar to Ref. [54]. As a result, the reconstructed track will not point to the interaction point and would therefore be unlikely to be considered a "good" track. In this case, the LEP constraints on charginos can be evaded. The light sbottom constraint can also be evaded by tuning appropriate mixing – see e.g. Refs. [30,55].
- For $m_\chi \gtrsim 100$ GeV, if the sbottom is decayed in more complicate modes other than $\tilde{b} \to b\chi$, the corresponding LHC bound on sbottom mass can be loosened.
- We can also work with heavier DM, e.g. $m_\chi = 300$ GeV, for example, as shown in Fig. 8. In this case, $m_{\tilde{b}} \lesssim 350$ GeV is consistent with the LHC searches, while the sbottom mediated process can give a significant contribution to spin-dependent scattering.

6. Conclusion

In this work, we have demonstrated the potential importance of the bottom quark contribution to the DM spin-dependent cross section due to the axial anomaly and resonant enhancement, which has hitherto been overlooked. Even though our calculation was carried out within the framework of the MSSM, the general conclusion will be relevant to any models with similar particle content, since the only relevant ingredients are χ, $\tilde{b}$ and the Z-boson.

In the MSSM, we calculated the bottom quark contribution to spin-dependent χ–p scattering. Firstly, we considered Gaugino DM, where there is no coupling between the Z-boson and DM. Assuming $m_\chi = 100$ GeV and degenerate first generation squarks with a mass of 1.5 TeV, we found that an sbottom of mass $m_{\tilde{b}} \lesssim 200$ GeV can give rise to a larger spin-dependent cross section for Wino DM. By contrast, for Bino DM a much lighter sbottom mass ($m_{\tilde{b}} \sim 110$ GeV) is required to give a competitive cross section. As for Higgsino DM, the first generation squark contributions are suppressed by their small Yukawa couplings. However, the Z-boson mediated process does contribute. For a given Higgsino mixing of DM the sbottom mediated process may interfere either constructively or destructively with Z-boson mediated processes, with different signs for protons and neutrons. For a typical mixing of Higgsino DM with mass around $\mathcal{O}$(10–100) GeV, we find that an sbottom of mass below 300 GeV can have non-negligible effects.

The squark mediated process that gives rise to an increase in spin-dependent DM scattering can also contribute to the spin-independent cross section. Our calculation shows that $\Delta(m_{\tilde{b}} - m_\chi) \gtrsim 50$ GeV is required to evade the LUX constraint for Wino DM, while for Higgsino DM,

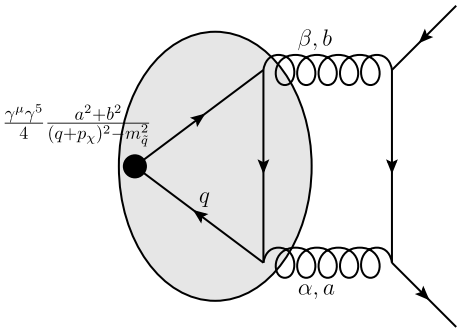

Fig. 9. Bottom quark contribution to the axial current.

either a small component of left-handed sbottom or a large cancellation in $\sigma_{\rm SI}$ is needed. Some incidental model dependent constraints from LEP and the LHC are considered as well. Those constraints, however, can be evaded in more general theoretical frameworks.

As pointed out earlier, our tree level results may break down as the sbottom and DM masses become degenerate ($\Delta(m_{\tilde{b}} - m_\chi) \lesssim 20$ GeV). We leave the higher order calculation for this small region for future work. Finally, while the calculations for the top quark case will be more complicated because there is no clear separation of mass scales for interesting ranges of DM mass, there is a clear need to investigate the role of the axial anomaly for that case too.

Acknowledgements

This work was supported by the Australian Research Council through the ARC Centre of Excellence for Particle Physics at the Terascale (Grant CE110001004) and by an ARC Australian Laureate Fellowship (Grant FL0992247, AWT).

Appendix A. Precision of tree level approximation

The heavy quark contributions to the axial charge start at two loop level through the process shown in Fig. 9. A detailed calculation of this diagram is given in Refs. [22,23]. In this study, all we need to know is the $m_{\tilde{q}}$ dependence of the amplitude. Then we can derive the range of $m_{\tilde{q}}$ for which the tree level effective coupling Eq. (16) is justified.

The $m_{\tilde{q}}$ dependence only exists in the triangle loop that is marked by the grey shaded ellipse in Fig. 9. The vertex amplitude is

$$\Gamma^{ab}_{\mu\alpha\beta} = \frac{a^2+b^2}{4}(-1)g^2\int\frac{d^4q}{(2\pi)^4}\mathrm{Tr}\{\frac{\gamma_\mu\gamma_5}{(q+p_\chi)^2-m_{\tilde{q}}^2}\cdot \frac{i}{\not{q}-m}(i\gamma_\alpha\frac{1}{2}\lambda^a)\frac{i}{\not{q}-m}(i\gamma_\beta\frac{1}{2}\lambda^b)\frac{i}{\not{q}-m}\}\,, \tag{A.1}$$

where m, q are the quark mass and momentum in the triangle, p_χ is the dark matter four momentum and $m_{\tilde{q}}$ is the squark mass. After introducing Feynman parameter x and the substitution:

$$l^\mu = q^\mu + xp^\mu_\chi\,, \tag{A.2}$$

$$\Delta = x^2p_\chi^2 - xp_\chi^2 + m^2(1-x) + xm_{\tilde{q}}^2\,, \tag{A.3}$$

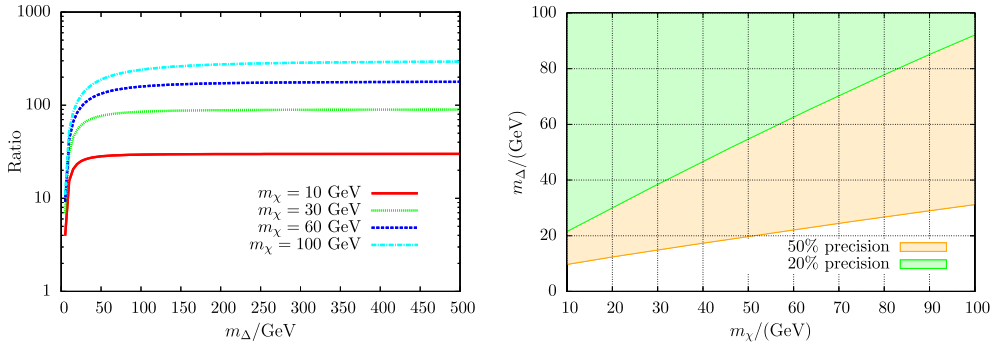

Fig. 10. Left: The m_Δ dependence of the ratio for several given DM masses. Right: In the shaded region, the tree level approximation matches the loop level results within required precision.

the vertex amplitude Eq. (A.1) can be simplified to

$$\Gamma^{ab}_{\mu\alpha\beta} \propto 3!\,\epsilon_{\alpha\beta\mu\rho}\int_0^1 dx\,\{-2x(p_\chi)_\sigma\int\frac{d^4l}{(2\pi)^4}\frac{l^\rho l^\sigma}{(l^2-\Delta)^4} - xp^\rho_\chi\cdot$$
$$\int\frac{d^4l}{(2\pi)^4}\frac{l^2}{(l^2-\Delta)^4} - xp^\rho_\chi(x^2p^2_\chi - m^2)\int\frac{d^4l}{(2\pi)^4}\frac{1}{(l^2-\Delta)^4}\,. \tag{A.4}$$

Finally, after integrating out the l^μ, we will get a simple $m_{\tilde{q}}$ and p_χ dependence of $\Gamma^{ab}_{\mu\alpha\beta}$:

$$\Gamma^{\text{loop}}(m_{\tilde{q}}, p_\chi) = \int_0^1 dx\left(\frac{3xp^\rho_\chi}{\Delta} - \frac{xp^\rho_\chi(x^2p^2_\chi - m^2)}{\Delta^2}\right) \tag{A.5}$$

On the other hand, the $m_{\tilde{q}}$ dependence of the tree level effective coupling can be factored out as

$$\Gamma^{\text{tree}} \propto \frac{1}{(m^2 - m^2_\chi)^2 - m^2_{\tilde{q}}}\,. \tag{A.6}$$

So we can define the ratio

$$\begin{aligned}\text{Ratio} &\propto \Gamma^{\text{loop}}/\,\Gamma^{\text{tree}}\\ &= ((m^2 - m^2_\chi)^2 - m^2_{\tilde{q}})\cdot\Gamma^{\text{loop}}(m_{\tilde{q}}, p_\chi)\,.\end{aligned} \tag{A.7}$$

Taking the non-relativistic limit for the DM momentum, i.e. $p_\chi = (m_\chi, 0, 0, 0)$, $m = m_b$ and $m_{\tilde{q}} = m_\Delta + m_\chi$, we solve the ratio numerically. The results are shown in the left panel of Fig. 10. From the figure we find that the ratio tends to a constant in the heavy squark region for given m_χ, which means the tree level description is accurate. While in the region of small mass splitting, the tree level results deviate from the full loop calculation considerably by a amount.

The range of m_Δ that permits the tree level approximation in required precision P can be solved by using the inequality

$$\text{Ratio}(m_\Delta)/\text{Ratio}(m_\Delta = 500) > (1 - P) \tag{A.8}$$

at each given DM mass. In the right panel of Fig. 10, we show the m_Δ region in which the tree level approximation matches the loop level result within 20% and 50% precision, respectively.

For example, when $m_\chi \sim 10$ GeV, $m_\Delta \gtrsim 20$ GeV is sufficient to guarantee that the tree level approximation is accurate within 20%.

References

[1] G. Bertone, D. Hooper, J. Silk, Particle dark matter: evidence, candidates and constraints, Phys. Rep. 405 (2005) 279–390, arXiv:hep-ph/0404175.
[2] WMAP Collaboration, E. Komatsu, et al., Seven-year Wilkinson Microwave Anisotropy Probe (WMAP) observations: cosmological interpretation, Astrophys. J. Suppl. Ser. 192 (2011) 18, arXiv:1001.4538.
[3] Planck Collaboration, P. Ade, et al., Planck 2013 results. XVI. Cosmological parameters, Astron. Astrophys. 571 (2014) A16, arXiv:1303.5076.
[4] DAMA Collaboration, LIBRA Collaboration, R. Bernabei, et al., New results from DAMA/LIBRA, Eur. Phys. J. C 67 (2010) 39–49, arXiv:1002.1028.
[5] CoGeNT Collaboration, C. Aalseth, et al., Results from a search for light-mass dark matter with a P-type point contact germanium detector, Phys. Rev. Lett. 106 (2011) 131301, arXiv:1002.4703.
[6] G. Angloher, M. Bauer, I. Bavykina, A. Bento, C. Bucci, et al., Results from 730 kg days of the CRESST-II dark matter search, Eur. Phys. J. C 72 (2012) 1971, arXiv:1109.0702.
[7] CDMS Collaboration, R. Agnese, et al., Silicon detector dark matter results from the final exposure of CDMS II, Phys. Rev. Lett. 111 (25) (2013) 251301, arXiv:1304.4279.
[8] XENON100 Collaboration, E. Aprile, et al., Dark matter results from 225 live days of XENON100 data, Phys. Rev. Lett. 109 (2012) 181301, arXiv:1207.5988.
[9] D.S. Akerib, et al., LUX Collaboration, Improved WIMP scattering limits from the LUX experiment, arXiv:1512.03506 [astro-ph.CO].
[10] R. Agnese, et al., SuperCDMS Collaboration, WIMP-search results from the second CDMSlite run, Phys. Rev. Lett. 116 (2016) 071301, http://dx.doi.org/10.1103/PhysRevLett.116.071301, arXiv:1509.02448 [astro-ph.CO].
[11] J.R. Ellis, R. Flores, Realistic predictions for the detection of supersymmetric dark matter, Nucl. Phys. B 307 (1988) 883.
[12] XENON100 Collaboration, E. Aprile, et al., Limits on spin-dependent WIMP-nucleon cross sections from 225 live days of XENON100 data, Phys. Rev. Lett. 111 (2) (2013) 021301, arXiv:1301.6620.
[13] M. Felizardo, T. Girard, T. Morlat, A. Fernandes, A. Ramos, et al., Final analysis and results of the phase II SIMPLE dark matter search, Phys. Rev. Lett. 108 (2012) 201302, arXiv:1106.3014.
[14] IceCube Collaboration, M. Aartsen, et al., Search for dark matter annihilations in the Sun with the 79-string IceCube detector, Phys. Rev. Lett. 110 (13) (2013) 131302, arXiv:1212.4097.
[15] S.D. Bass, R.J. Crewther, F.M. Steffens, A.W. Thomas, Phys. Rev. D 66 (2002) 031901, arXiv:hep-ph/0207071.
[16] T. Appelquist, J. Carazzone, Phys. Rev. D 11 (1975) 2856.
[17] S.L. Adler, Phys. Rev. 177 (1969) 2426.
[18] R.J. Crewther, N.K. Nielsen, Nucl. Phys. B 87 (1975) 52.
[19] J.C. Collins, F. Wilczek, A. Zee, Phys. Rev. D 18 (1978) 242.
[20] D.B. Kaplan, A. Manohar, Nucl. Phys. B 310 (1988) 527.
[21] R.D. Carlitz, J.C. Collins, A.H. Mueller, The role of the axial anomaly in measuring spin dependent parton distributions, Phys. Lett. B 214 (1988) 229.
[22] S.D. Bass, R.J. Crewther, F.M. Steffens, A.W. Thomas, Running couplings for the simultaneous decoupling of heavy quarks, Phys. Lett. B 634 (2006) 249–254, arXiv:hep-ph/0507278.
[23] R.J. Crewther, S.D. Bass, F.M. Steffens, A.W. Thomas, Decoupling heavy particles simultaneously, Nucl. Phys. B, Proc. Suppl. 141 (2005) 159–164, arXiv:hep-ph/0601244.
[24] H. Nilles, Supersymmetry, supergravity and particle physics, Phys. Rep. 110 (1–2) (1984) 1–162.
[25] H. Haber, G. Kane, The search for supersymmetry: probing physics beyond the standard model, Phys. Rep. 117 (2–4) (1985) 75–263.
[26] ATLAS, https://twiki.cern.ch/twiki/bin/view/AtlasPublic/SupersymmetryPublicResults.
[27] CMS, https://twiki.cern.ch/twiki/bin/view/CMSPublic/PhysicsResultsSUS.
[28] R. Barbieri, G. Giudice, Upper bounds on supersymmetric particle masses, Nucl. Phys. B 306 (1988) 63.
[29] J.R. Ellis, K. Enqvist, D.V. Nanopoulos, F. Zwirner, Observables in low-energy superstring models, Mod. Phys. Lett. A 1 (1986) 57.
[30] B. Batell, C.E.M. Wagner, L.-T. Wang, Constraints on a very light sbottom, J. High Energy Phys. 1405 (2014) 002, arXiv:1312.2590.

[31] J. Abdallah, A. Ashkenazi, A. Boveia, G. Busoni, A. De Simone, et al., Simplified models for dark matter and missing energy searches at the LHC, arXiv:1409.2893.
[32] B. Batell, J. Pradler, M. Spannowsky, Dark matter from minimal flavor violation, J. High Energy Phys. 1108 (2011) 038, arXiv:1105.1781.
[33] P. Agrawal, S. Blanchet, Z. Chacko, C. Kilic, Flavored dark matter, and its implications for direct detection and colliders, Phys. Rev. D 86 (2012) 055002, arXiv:1109.3516.
[34] P. Agrawal, B. Batell, D. Hooper, T. Lin, Flavored dark matter and the galactic center gamma-ray excess, Phys. Rev. D 90 (6) (2014) 063512, arXiv:1404.1373.
[35] G.S. Bali, et al., QCDSF Collaboration, Phys. Rev. Lett. 108 (2012) 222001, arXiv:1112.3354 [hep-lat].
[36] J. Rosiek, Complete set of Feynman rules for the MSSM: erratum, arXiv:hep-ph/9511250.
[37] L. Vietze, P. Klos, J. Menéndez, W.C. Haxton, A. Schwenk, Phys. Rev. D 91 (4) (2015) 043520, arXiv:1412.6091 [nucl-th].
[38] K. Griest, Calculations of rates for direct detection of neutralino dark matter, Phys. Rev. Lett. 61 (1988) 666–669.
[39] K. Griest, Cross-sections, relic abundance and detection rates for neutralino dark matter, Phys. Rev. D 38 (1988) 2357.
[40] M. Drees, M. Nojiri, Neutralino–nucleon scattering revisited, Phys. Rev. D 48 (1993) 3483–3501, arXiv:hep-ph/9307208.
[41] J. Hisano, K. Ishiwata, N. Nagata, Gluon contribution to the dark matter direct detection, Phys. Rev. D 82 (2010) 115007, arXiv:1007.2601.
[42] H. Ohki, H. Fukaya, S. Hashimoto, T. Kaneko, H. Matsufuru, et al., Nucleon sigma term and strange quark content from lattice QCD with exact chiral symmetry, Phys. Rev. D 78 (2008) 054502, arXiv:0806.4744.
[43] J. Giedt, A.W. Thomas, R.D. Young, Dark matter, the CMSSM and lattice QCD, Phys. Rev. Lett. 103 (2009) 201802, arXiv:0907.4177.
[44] R.D. Young, A.W. Thomas, Phys. Rev. D 81 (2010) 014503, arXiv:0901.3310 [hep-lat].
[45] P.E. Shanahan, A.W. Thomas, R.D. Young, Phys. Rev. D 87 (2013) 074503, arXiv:1205.5365 [nucl-th].
[46] J. Pumplin, D. Stump, J. Huston, H. Lai, P.M. Nadolsky, et al., New generation of parton distributions with uncertainties from global QCD analysis, J. High Energy Phys. 0207 (2002) 012, arXiv:hep-ph/0201195.
[47] P. Gondolo, S. Scopel, On the sbottom resonance in dark matter scattering, J. Cosmol. Astropart. Phys. 1310 (2013) 032, arXiv:1307.4481.
[48] G. Belanger, F. Boudjema, A. Pukhov, A. Semenov, Dark matter direct detection rate in a generic model with micrOMEGAs 2.2, Comput. Phys. Commun. 180 (2009) 747–767, arXiv:0803.2360.
[49] G. Belanger, F. Boudjema, A. Pukhov, A. Semenov, micrOMEGAs_3: a program for calculating dark matter observables, Comput. Phys. Commun. 185 (2014) 960–985, arXiv:1305.0237.
[50] ALEPH Collaboration, A. Heister, et al., Search for charginos nearly mass degenerate with the lightest neutralino in e^+e^- collisions at center-of-mass energies up to 209-GeV, Phys. Lett. B 533 (2002) 223–236, arXiv:hep-ex/0203020.
[51] ATLAS Collaboration, G. Aad, et al., Search for direct third-generation squark pair production in final states with missing transverse momentum and two b-jets in $\sqrt{s} = 8$ TeV pp collisions with the ATLAS detector, J. High Energy Phys. 1310 (2013) 189, arXiv:1308.2631.
[52] ATLAS Collaboration, Search for bottom squark pair production with the ATLAS detector in proton–proton collisions at $\sqrt{s} = 13$ TeV, ATLAS-CONF-2015-066.
[53] G. Aad, et al., ATLAS Collaboration, Search for pair-produced third-generation squarks decaying via charm quarks or in compressed supersymmetric scenarios in pp collisions at $\sqrt{s} = 8$ TeV with the ATLAS detector, Phys. Rev. D 90 (5) (2014) 052008, http://dx.doi.org/10.1103/PhysRevD.90.052008, arXiv:1407.0608 [hep-ex].
[54] B. Batell, S. Jung, C.E. Wagner, Very light charginos and Higgs decays, J. High Energy Phys. 1312 (2013) 075, arXiv:1309.2297.
[55] T. Han, Z. Liu, S. Su, Light neutralino dark matter: direct/indirect detection and collider searches, J. High Energy Phys. 1408 (2014) 093, arXiv:1406.1181.